Cancer and Metastasis Reviews **17:** 271–277, 1999.

Orthotopic transplant mouse models with green fluorescent protein-expressing cancer cells to visualize metastasis and angiogenesis

Robert M. Hoffman
AntiCancer, Inc., San Diego, CA, USA; Department of Surgery, UCSD Medical Center, San Diego, CA, USA

Key words: metastasis, orthotopic, intact tissue, implantation, GFP, nude mice

Summary

There have been major efforts in metastasis research in recent years, especially on the role of angiogenesis in the metastatic process. Much of the information in this area has been obtained from model systems that are not representative of clinical cancer. The technique of surgical orthotopic implantation (SOI) has allowed the development of clinically relevant metastatic models of human cancer in immunodeficient rodents such as the nude and SCID mouse. In order to allow direct visualization of the metastatic process, we took advantage of the green fluorescent protein (GFP) of the jellyfish, *Aequorea victoria*. A series of cancer cell lines have been stably transfected with vectors containing humanized GFP cDNA. To utilize GFP expression for metastasis studies, fragments of subcutaneously growing tumor, which were comprised of GFP-expressing cells, were implanted by SOI in nude mice. Subsequent metastases were visualized in systemic organs by GFP fluorescence in the lung, liver, bones, brain and other organs down to the single-cell level. With this fluorescent tool, we detected and visualized for the first time tumor cells at the microscopic level in fresh viable tissue in their normal host organs even in the live animal. Angiogenesis is readily visualized in the transplanted GFP-expressing tumors in real time *in situ* in the live animal using simple laparotomy and fluorescent techniques. The results with the GFP-transfected tumor cells, combined with the use of SOI, demonstrate a fundamental advance to visualize and study cancer metastasis and the role of angiogenesis and other factors in the metastatic process.

Introduction

There has been a great interest in the study of metastasis in recent years, especially in the role of angiogenesis in metastasis. Recent results have indicated however, that the choice of animal models is critical for obtaining relevant data on the control of metastasis and the role of angiogenesis and other factors in the metastatic process. Fidler [1] and others have demonstrated the importance of orthotopic transplantation of tumors in appropriate recipients such as nude or SCID mice. The orthotopic site provides the relevant tumors microenvironment [1] for metastasis in contrast to ectopic sites such as the subcutaneous space or even related organs [2]. We have developed the technique of surgical orthotopic implantation (SOI) of histologically intact tumor tissue fragments for clinically relevant metastatic models of human cancer in immunodeficient rodents such as the nude and SCID mouse [3–8].

SOI has been shown by Cowen et al. [9] to be critical for a functional network of vessels to form in liver metastasis from a colon tumor. In contrast, iv injection of tumor cells results in undifferentiated tumor deposits in the lung and liver of the nude mouse without stromal or vascular involvement [9]. The importance of SOI on resulting metastasis and angiogenesis becomes of particular importance with regard to the accurate pre-clinical evaluation of new antiangiogenesis agents whose development thus far has depended on animals that were injected ectopically with suspensions of tumor cells [10–16]. This has been demonstrated in an SOI model of colon cancer where an antiangiogenic agent inhibited colon cancer metastasis but not the primary tumor growth [34].

The early stages of tumor progression and micrometastasis formation have been difficult to analyze due to the inability to identify small numbers of tumor cells against a background of many host cells. For example, the visualization of tumor cell emboli, micrometastases and their progression over real-time during the course of the disease has been difficult to study in current models of metastasis. Previous studies used transfection of tumor cells with the *Escherichia coli* beta-galactosidase (lacZ) gene to detect micrometastases [17,18]. However, detection of lacZ requires extensive histological preparation, and therefore it is not possible to detect and visualize tumor cells in viable fresh tissue or the live animal at the microscopic level. The visualization of tumor invasion and micrometastasis formation in viable fresh tissue or the live animal is necessary for a critical understanding of tumor progression and its control.

To enhance the resolution of the visualization of micrometastases in fresh tissue, we have utilized the green fluorescent protein (GFP) gene, cloned from the bioluminescent jellyfish *Aequorea victoria* [19]. GFP has demonstrated its potential for use as a marker for gene expression in a variety of cell types [20,21]. The GFP cDNA encodes a 283 amino acid polypeptide with molecular weight of 27 kD [22,23]. The monomeric GFP requires no other *Aequorea* proteins, substrates, or cofactors to fluoresce [24]. Recently, GFP gene gain-of-function mutants have been generated by various techniques [25–28]. For example, the GFP-S65T clone has the serine-65 codon substituted with a threonine codon which results in a single excitation peak at 490 nm [25]. Moreover, to develop higher expression in human and other mammalian cells, a humanized hGFP-S65T clone was isolated [29]. The much brighter fluorescence in the mutant clones allows for easy detection of GFP expression in transfected cells.

We have demonstrated the isolation of stable transfectants of human lung carcinoma cells (ANIP 973 and H-460) and Chinese hamster ovary (CHO) cells that express high-level GFP fluorescence *in vitro* [30-35] and a series of cell lines from the National Cancer Institute (NCI) cell line screen (H460, colon cancer Colo-205, prostate cancer PC-3 and DU-145, breast cancer MDA-MB435 and MDA-MB468, kidney cancer SN12C, tongue cancer SCC-25, melanoma LOX). The transfectants are highly fluorescent *in vivo* in tumors formed from the cells. Using these fluorescent transfectants, orthotopic-transplant animal models [3–8] were utilized for visualizing the metastatic and angiogenic processes in fresh tissue including living animals that heretofore was not possible [30–35].

These developments with GFP-expressing tumor cells provide an invaluable new tool for understanding the most important steps in tumor host-organ interaction, tumor progression, metastasis, and angiogenesis.

Materials and methods

DNA manipulations and expression vector constructions

The dicistronic expression vector (pED-mtx^r) was obtained from Genetics Institute (Cambridge, MA) [33]. The expression vector containing the codon-optimized hGFP-S65T gene was purchased from CLONTECH Laboratories, Inc. (Palo Alto, CA). To construct the hGFP-S65T containing expression vector, phGFP-S65T was digested with Hin*d* III, blunted at the end. The entire hGFP coding region was then excised with X*ba* I. The pED-mtx^r vector was digested with P*st* I, blunted at the end, and further digested with X*ba* I. The hGFP-S65T cDNA fragment was then unidirectionally subcloned into pED-mtx^r.

Cell culture, transfection, selection

CHO-K1 cells were cultured in DMEM (GIBCO) containing 10% fetal calf serum (FCS) (Gemini Bio-products, Calabasas, CA), 2 mM L-gulutamine and 100 μM non-essential amino acids (Irvine Scientific, Santa Ana, CA). ANIP 973 cells and the NCI cell lines were cultured either in MEM (GIBCO), RPMI 1640 (GIBCO) or Ham's F-12 (Irvine Scientific) containing 10% fetal calf serum (FCS) (Gemini Bio-products, Calabasas, CA).

For transfection, near-confluent CHO-K1 or ANIP cells were incubated with a precipitated mixture of LipofectAMINE™ reagent (GIBCO), and saturating amounts of plasmids for 6 h before being replenished with fresh medium.

NCI cell lines were transfected with the pLEIN retrovirus containing the EGFP gene (Clontech) using DOTAB liposome transfection reagent (Boerhinger Mannheim). pLEIN expresses EGFP and the neomycin gene on the same bicistronic message [35].

CHO-K1 cells and ANIP were harvested by trypsin/EDTA 48 h post-transfection, and subcultured at a ratio of 1 : 15 into selective medium which

contained various concentrations of methotrexate (MTX) up to 1.5 μM. Cells with stably integrated plasmids were selected by growing transiently-transfected cells in medium with increasing concentrations of MTX. Clones were isolated with cloning cylinders (Bel-Art Products, Pequannock, NJ) with trypsin/EDTA. They were amplified and transferred with conventional culture methods. CHO Clone-38 and ANIP Clone-26 were chosen because of their high-intensity GFP fluorescence and stability.

GFP-transfected NCI cell lines were similarly selected but with neomycin (0.5–2 μg/ml) [35].

Surgical orthotopic implantation of CHO-K1 Clone-38 in nude mice

Tumor fragments (1 mm^3) derived from the nude mouse subcutaneous CHO-K1 Clone-38 tumor were implanted by surgical orthotopic implantation (SOI) on the ovarian serosa in six nude mice [5]. The mice were anesthetized by isofluran inhalation. An incision was made through the left lower abdominal pararectal line and peritoneum. The left ovary was exposed and part of the serosal membrane was scraped with a forceps. Four 1 mm^3 tumor pieces were fixed on the scraped site of the serosal surface with an 8-0 nylon suture (Look, Norwell, MA). The ovary was then returned into the peritoneal cavity, and the abdominal wall and the skin were closed with 6-0 silk sutures. Four weeks later, the mice were sacrificed and the lungs and the other organs were removed.

Surgical orthotopic implantation of ANIP 973 human lung cancer in nude mice

Tumor pieces (1-mm^3) derived from the nude mouse subcutaneous tumor formed from ANIP Clone-26 were implanted by surgical orthotopic implantation (SOI) onto the left visceral pleura in four nude mice [4]. The mice were anesthetized by Isofluran inhalation. A small 1-cm transverse incision was made on the left-lateral chest of the nude mice via the fourth intercostal space. A small incision provided access to the pleural space, and resulted in total lung collapse. Five tumor pieces were sewn together with a 8-0 nylon (Look, Norwell, MA) surgical suture and fixed by making one knot. The lung was taken up by forceps and the tumor sewn into the lower part of the lung with one suture. The lung tissue was then returned into the chest cavity. The chest muscles and skin were closed with a single layer of 6-0 silk sutures. The lung was reinflated by withdrawing air from the chest cavity with a 23-gauge needle.

Surgical orthotopic implantation of GFP-transfected PC-3 in the prostate of nude mice was carried out as described [8]. Surgical orthotopic implantation of GFP-transfected H460 was carried out in similar fashion as for ANIP-973 described above.

Tumor angiogenesis visualization in live animals with GFP tumors

Angiogenesis of GFP tumors was visualized in live animals by injection of 200 μl of 0.1 μM rhodamine five minutes before surgical exploration. A GFP filter set with an excitation band-pass filter (D425/60) and for emission, a long pass filter (GG475) (Chroma Technology, Brattleboro, UT) was used for fluorescence with a Leica Stereo Microscope.

Results and discussion

Isolation of stable high-level expression GFP transfectants of CHO-K1 and ANIP cells

The expression-vector transfected CHO-K1 and ANIP cells were able to grow in levels of MTX up to 1.5 μM. The selected MTX resistant CHO and ANIP cells had a striking increase in GFP fluorescence compared to the transiently-transfected cells. A subclone was termed CHO-K1 GFP 38 (Clone-38) which was stable in 1.5 μM MTX, possibly due to chromosomal integration of the amplified GFP genes [30]. There was no difference in the cell proliferation rates of parental cells and selected transfectants determined by comparing their doubling times. A subclone of ANIP 973 which expressed the strongest GFP was isolated and termed ANIP 973-hGFP-S65T-Clone-26 (Clone 26) [31].

Patterns of metastasis of ovarian tumor after SOI visualized by GFP

Nude mice were implanted with 1-mm^3 cubes of CHO-K1 Clone-38 tumor into the ovary and were sacrificed at four weeks [30]. All mice had tumors in the ovaries. The tumor had also seeded throughout the peritoneal cavity, including the colon, cecum, small intestine, spleen, and peritoneal wall. The primary tumor and peritoneal metastases were strongly fluorescent. Numerous micrometastases were detected by fluorescence on the

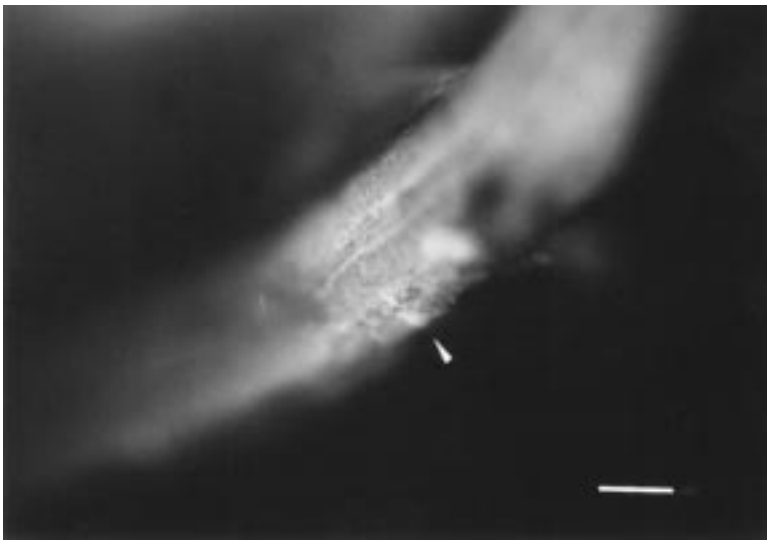

Figure 1. Ribmetastasis of GFP-expressing human prostate PC-3 tumor (arrow) after surgical orthotopic transplantation (Bar = 200 μM).

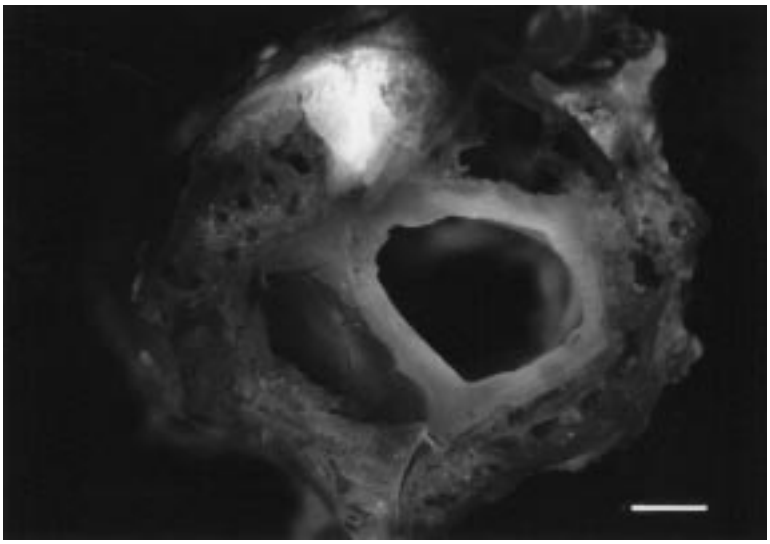

Figure 2. Metastasis of GFP-expressing human lung cancer human lung H460 tumor to the spine after SOI to a nude mouse (Bar = 325 μM).

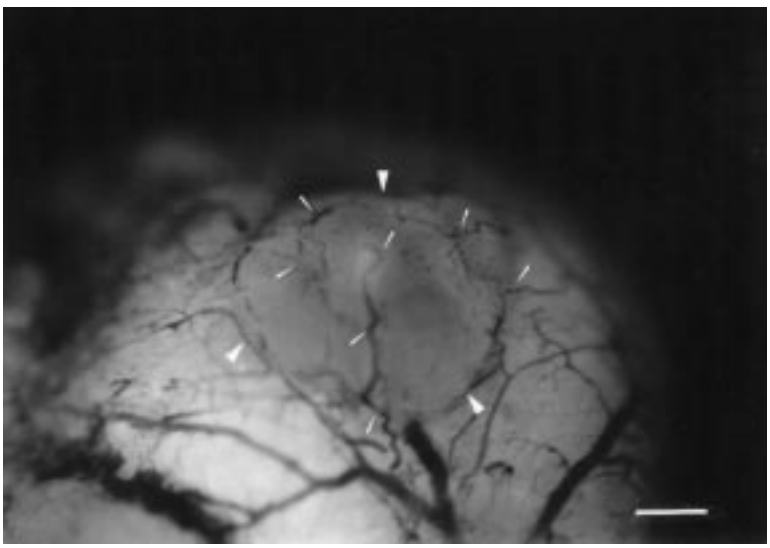

Figure 3. Angiogenesis visualized in GFP-expressing ANIP-973 human lung tumor cells growing on the wall of the nude mouse colon after injection of rhodamine dye (see Materials and methods for detail). Thick arrows denote perimeter of tumor. Thin arrows denote tumor blood vessels. (Bar = 200 μM).

lungs of all mice. Multiple micrometastasis were also detected by fluorescence on the liver, kidney, contralateral ovary, adrenal gland, para-aortic lymph node, and pleural membrane down to the single-cell level. Single-cell micrometastases could not be detected by standard histological techniques. Even these multiple-cell small colonies were difficult to detect by hematoxylin and eosin staining, but could be detected and visualized clearly by GFP-fluorescence.

Patterns of metastasis of lung tumor after SOI visualized by GFP expression

Primary tumors grew in the operated left lung in all mice after SOI of GFP-transfected ANIP 973 Clone-26. GFP expression allowed visualization of the advancing margin of the tumor spreading in the ipsilateral lung. All animals explored had evidence of chest wall invasion and local and regional spread. Metastatic contralateral tumors involved the mediastinum, contralateral pleural cavity, the contralateral visceral pleura, occurring in all mice. While, the ipsilateral tumor had a continuous and advancing margin, the contralateral tumor seemed to have been formed by multiple seeding events. These observations were made possible by GFP fluorescence of the fresh tumors tissue [31,32]. When non-GFP-transfected ANIP was compared with GFP-transformed ANIP for metastatic capability similar results were seen [31]. Contralateral hilar lymph nodes were also involved shown by GFP expression. A cervical lymph node metastasis was brightly visualized by GFP in fresh tissue [31,32].

GFP-PC-3 transplanted by SOI in the prostate demonstrated extremely high malignancy with seeding in the liver, lung, skull, bones (Figure 1) and brain [35]. GFP H460 transplanted by SOI in the lung demonstrated extensive bone metastasis throughout the skeleton (Figure 2) and metastasis in many other organs [35].

To study tumor progression and the metastatic process at the earliest stages, it was important to use a metastatic model which could allow spontaneous metastasis in the animal. In the last 10 years, it has become clear that orthotopic sites of implantation are critical for the metastatic expression of transplanted tumors in nude mice. We have found that the use of tissue fragments rather than dispersed cells allows full expression of the metastatic capability of surgically orthotopically implanted (SOI) tumors [3–8]. GFP-gene-transfected CHO-K1 Clone-38 cells were successfully used to visualize extensive peritoneal seeding as well as distant macro- and micro-metastases in nude mice including the lung following SOI in the ovary of subcutaneous tumor fragments. We utilized the SOI model and GFP-expressing ANIP Clone-26 tumor to visualize human lung tumor growth and metastases to the mediastinum and contralateral lung, as well as to lymph nodes. PC-3 and H460 have high bone metastatic capability as visualized with GFP. These are very important clinical events and can now be visualized much more realistically by GFP in fresh tissue. These models provided the opportunity to demonstrate the capability of GFP for detection and visualization of metastases.

We have visualized actively colonizing as well as dormant tumor cells in the lung and brain. Dormant micrometastasis is one of the most important steps to understand in tumor progression [34]. In recent studies, the mechanism of this important phenomenon was studied with regard to angiogenesis and other chemical regulators of tumor colonization [34,10–16]. However, these experimental models did not allow direct observation of the dormant colonies in fresh live tissue or the live animal as can be done with GFP-expressing tumor cells.

The GFP-expressing tumors have been shown to be useful for visualization of early to late stage angiogenesis in the living animal (Yang and Hoffman, unpublished results). Each tumor deposit can be observed for extent of angiogenesis over time by surgical exploration with fluorescence microscopy (Figure 3). Results thus far suggest site and tumor type influence the extent and apparent dependence on angiogenesis for tumor expansion (Yang and Hoffman, unpublished results).

The methods described in this review, SOI and GFP expression, will facilitate the understanding of tumor growth and progression including seeding and target organ colonization and the role of angiogenesis in this process. These studies should provide new insights into metastatic mechanisms, and evaluation of new agents for treatment of metastatic disease.

References

1. Fidler IJ: Critical factors in the biology of human cancer metastasis. Cancer Res 50: 6130–6138, 1990
2. Togo S, Shimada H, Kubota T, Moossa AR, Hoffman RM: Host organ specifically determines cancer progression. Cancer Res 55: 681–684, 1995

3. Astoul P, Colt HG, Wang X, Hoffman RM: A 'patient-like' nude mouse model of parietal pleural human lung adenocarcinoma. Anticancer Res 14: 85–92, 1994
4. Wang X, Fu X, Hoffman RM: A new patient-like metastatic model of human lung cancer constructed orthotopically with intact tissue via thoracotomy in immunodeficient mice. Int J Cancer 51: 992–995, 1992
5. Fu X, Hoffman RM: Human ovarian carcinoma metastatic models constructed in nude mice by orthotopic transplantation of histologically-intact patient specimens. Anticancer Res 13: 283–286, 1993
6. Hoffman RM: Orthotopic is orthodox: Why are orthotopic-transplant metastatic models different from all other models? J Cellular Biochem 56: 1–3, 1994
7. Kuo T, Kubota T, Watanabe M, Furukawa T, Teramoto T, Ishibiki K, Kitajima M, Moossa AR, Penman S, Hoffman RM: Liver colonization competence governs colon cancer metastasis. Proc Natl Acad Sci USA 92: 12085–12089, 1995
8. An Z, Wang X, Geller J, Moossa AR, Hoffman RM: Surgical orthotopic implantation allows high lung and lymph node metastatic expression of human prostate carcinoma cell line PC-3 in nude mice. The Prostate 34: 169–174, 1998
9. Cowen SE, Bibby MC, Double JA: Characterisation of the vasculature within a murine adenocarcinoma growing in different sites to evaluate the potential of vascular therapies. Acta Oncologica 34: 357–360, 1995
10. O'Reilly MS, Holmgren L, Shing Y, Chen C, Rosenthal RA, Moses M, Lane WS, Cao Y, Sage EH, Folkman J: Angiostatin: A novel angiogenesis inhibitor that mediates the suppression of metastases by a Lewis lung carcinoma. Cell 79: 315–328, 1994
11. O'Reilly MS, Holmgren L, Chen C, Folkman J: Angiostatin induces and sustains dormancy of human primary tumors in mice. Nature Med 2: 689–692, 1996
12. Folkman J: Angiogenesis in cancer, vascular, rheumatoid and other diseases. Nature Med 1: 27–31, 1995
13. O'Reilly MS, Boehm T, Shing Y, Fukai N, Vasios G, Lane WS, Flynn E, Birkhead JR, Olsen BR, Folkman J: Endostatin: An endogenous inhibitor of angiogenesis and tumor growth. Cell 88: 277–285, 1997
14. Boehm T, Folkman J, Browder T, O'Reilly MS: Antiangiogenesis therapy of experimental cancer does not induce acquired drug resistance. Nature 390: 404–407, 1997
15. Arap W, Pasqualini R, Ruoslahti E: Cancer treatment by targeted drug delivery to tumor vasculature in a mouse model. Science 279: 377–380, 1998
16. Pasqualini R, Koivunen E, Ruoslahti E: αv integrins as receptors for tumor targeting by circulating ligands. Nature Biotech 15: 542–546, 1997
17. Lin WC, Pretlow TP, Pretlow TG, Culp LA: Bacterial *lac*Z gene as a highly sensitive marker to detect micrometastasis formation during tumor progression. Cancer Res 50: 2808–2817, 1990
18. Lin WC, Culp LA: Altered establishment/clearance mechanisms during experimental micrometastasis with live and/or disabled bacterial lacZ-tagged tumor cells. Invasion Metas 12: 197–209, 1992
19. Morin J, Hastings J: Energy transfer in a bioluminescent system. J Cell Physiol 77: 313–318, 1972
20. Chalfie M, Tu Y, Euskirchen G, Ward WW, Prasher DC: Green fluorescent protein as a marker for gene expression. Science 263: 802–805, 1994
21. Cheng L, Fu J, Tsukamoto A, Hawley RG: Use of green fluorescent protein variants to monitor gene transfer and expression in mammalian cells. Nature Biotech 14: 606–609, 1996
22. Prasher DC, Eckenrode VK, Ward WW, Prendergast FG, Cormier MJ: Primary structure of the *Aequorea victoria* green-fluorescent protein. Gene 111: 229–233, 1992
23. Yang F, Miss LG, Phillips GN Jr: The molecular structure of green fluorescent protein. Nature Biotech 14: 1252–1256, 1996
24. Cody CW, Prasher DC, Welstler VM, Prendergast FG, Ward WW: Chemical structure of the hexapeptide chromophore of the *Aequorea* green fluorescent protein. Biochemistry 32: 1212–1218, 1993
25. Heim R, Cubitt AB, Tsien RY: Improved green fluorescence. Nature 373: 663–664, 1995
26. Delagrave S, Hawtin RE, Silva CM, Yang MM, Youvan DC: Red-shifted excitation mutants of the green fluorescent protein. Bio/Technology 13: 151–154, 1995
27. Cormack B, Valdivia R, Falkow S: FACS-optimized mutants of the green fluorescent protein (GFP). Gene 173: 33–38, 1996
28. Cramer A, Whitehorn EA, Tate E, Stemmer WPC: Improved green fluorescent protein by molecular evolution using DNA shuffling. Nature Biotech 14: 315–319, 1996
29. Zolotukhin S, Potter M, Hauswirth WW, Guy J, Muzycka N: 'Humanized' green fluorescent protein cDNA adapted for high-level expression in mammalian cells. J Virology 70: 4646–4654, 1996
30. Chishima T, Miyagi Y, Wang X, Yamaoka H, Shimada H, Moossa AR, Hoffman RM: Cancer invasion and micrometastasis visualized in live tissue by green fluorescent protein expression. Cancer Research 57: 2042–2047, 1997
31. Chishima T, Miyagi Y, Wang X, Baranov E, Tan Y, Shimada H, Moossa AR, Hoffman RM: Metastatic patterns of lung cancer visualized live and in process by green fluorescence protein expression. Clin Exper Metas 15: 547–552, 1997
32. Chishima T, Miyagi Y, Wang X, Tan Y, Shimada H, Moossa AR, Hoffman RM: Visualization of the metastatic process by green fluorescent protein expression. Anticancer Res 17: 2377–2384, 1997
33. Kaufman RJ, Davies MV, Wasley LC, Michnick D: Improved vectors for stable expression of foreign genes in mammalian cells by use of the untranslated leader sequence from EMC virus. Nucleic Acids Res 19: 4485–4490, 1991
34. Holmgren L, O'Reilly MS, Folkman J: Dormancy of micrometastases: Balanced proliferation and apoptosis in the presence of angiogenesis suppression. Nature Med 1: 149–153, 1995
35. Yang M, Hasegawa S, Jiang P, Wang X, Tan Y, Chishima T, Shimada H, Moossa AR and Hoffman RM: Widespread skeletal metastatic potential of human lung cancer revealed by green fluorescent protein expression. Cancer Res 58: 4217–4221, 1998

36. Tanaka T, Konnott, Matsuda I, Nakamura S, and Baba S: Prevention of hepatic metastasis of human colon cancer by angiogenesis inhibition TNP-470. Cancer Res 55: 836–839, 1995

Address for offprints: Robert M. Hoffman, AntiCancer, Inc., 7917 Ostrow Street, San Diego, CA 92111. *Tel*: 619-654-2555; *Fax*: 619-268-4175; *e-mail*: all@anticancer.com